Transcriptome analysis revealed the new mechanism of the intra-myocardial injectable alginate-hydrogel in the treatment of ventricular function degradation

Huiyong Wang[1,2#], Ting Zhou[1#], Wentao Ma[1,3#], Ji Zheng[4], Zhiyong Cao[5], Caiyun He[2], Pedro A. Lemos[6,7], Jianfang Luo[1,3]

[1]Department of Cardiology, Guangdong Provincial People's Hospital (Guangdong Academy of Medical Sciences), Southern Medical University, Guangzhou, China; [2]Department of Cardiology, The First Affiliated Hospital of Guangzhou Medical University, Guangzhou, China; [3]School of Medicine, South China University of Technology, Guangzhou, China; [4]Hangzhou Deke Medtech Co., Ltd., Hangzhou, China; [5]Suzhou NGGT Biotechnology Co., Ltd., Suzhou, China; [6]Department of Cardiology, Hospital Israelita Albert Einstein, Sao Paulo, SP, Brazil; [7]Department of Cardiology, Heart Institute-InCor, University of Sao Paulo Medical School, Sao Paulo, SP, Brazil

Contributions: (I) Conception and design: H Wang, J Luo; (II) Administrative support: J Luo; (III) Provision of study materials or patients: H Wang, T Zhou, W Ma; (IV) Collection and assembly of data: J Zheng, Z Cao, C He; (V) Data analysis and interpretation: H Wang, T Zhou, W Ma, J Zheng, Z Cao; (VI) Manuscript writing: All authors; (VII) Final approval of manuscript: All authors.

[#]These authors contributed equally to this work.

Correspondence to: Jianfang Luo, MD, PhD. Department of Cardiology, Guangdong Provincial People's Hospital (Guangdong Academy of Medical Sciences), Southern Medical University, Guangzhou, China; School of Medicine, South China University of Technology, #106 Zhongshan Road II, Yuexiu District, Guangzhou 510080, China. Email: jianfangluo@sina.com.

Background: Myocardial infarction (MI) is one of the most lethal cardiovascular diseases. The loss of cardiomyocytes and the degradation of the extracellular matrix leads to high ventricular wall stress, which further drives the pathological thinning of the ventricular wall during MI. Injecting biomaterials to thicken the infarct ventricular wall provides mechanical support, thereby inhibiting the continued expansion of the heart. As an injectable biomaterial, alginate hydrogel has achieved exciting results in clinical trials, but further research needs to be conducted to determine whether it can improve cardiac function in addition to providing mechanical support. This study sought to explore these mechanisms in an animal model of MI.

Methods: A MI model was established in male C57BL/6J mice by ligation of the proximal left anterior descending (LAD) coronary artery. Intramyocardial injections (hydrogel or saline group) were performed in the proximal wall regions bordering the infarct area (with one 20-μL injection). Four weeks after MI, RNA sequencing revealed that 342 messenger RNAs (mRNAs) from the infarcted hearts were differentially expressed between the saline group and hydrogel group. We subsequently conducted a Gene Ontology (GO) and Kyoto Encyclopedia of Genes and Genomes (KEGG) pathway analysis to analyze the RNA sequencing data. In addition, we employed both western blotting and quantitative reverse transcriptase polymerase chain reaction (qRT-PCR) techniques to verify a number of genes that were differentially expressed and could potentially affect cardiac function after MI. Subsequently, we confirmed these findings through *in vitro* experiments.

Results: We found that compared with hydrogel treatment group, 250 mRNAs were upregulated and 92 mRNAs were downregulated in saline group (P<0.05). And by exploring the GO and KEGG signaling pathways as well as the protein-protein interaction (PPI) network, we found that administration of alginate hydrogel modulated cardiomyocyte inflammation-associated proteins as well as chemokine-related proteins during the inflammatory response phase after MI. In addition, our analysis at both the protein and RNA level revealed that *B2M* was effective in improving cardiac function after MI in the hydrogel treatment group, which was consistent in the myocardium oxygen and glucose deprivation (OGD) injury model.

Conclusions: We explored the transcriptome changes of infarcted hearts after alginate-hydrogel injection during the inflammatory response period. Our findings suggest that the injectable hydrogel directly alters

---

the inflammatory response and the chemokine-mediated signaling pathway of cardiomyocytes, ultimately improving cardiac function.

Introduction

Myocardial infarction (MI) has been one of the most common cardiovascular diseases and a leading cause of death worldwide for decades (1). Myocardial cell death, the fibrosis of infarcted myocardial tissue, and compensatory hypertrophy of the residual myocardium also lead to heart failure and death after MI (2-5).

Vascular reconstruction in the early stages of MI through drug therapy, medical device implantation, and organ transplantation aim to improve patients' short- and long-term prognoses and reduce the risk of cardiovascular complications (6). Due to the disadvantages of blood clots, poor immune rejection, and a limited number of donor organs, individuals who survive the initial event often die due to arrhythmias and slow mechanical damage that progressively deteriorates heart function and eventually leads to end-stage heart failure (7). Loss of cardiomyocytes and the subsequent degradation of the extracellular matrix due to inflammation lead to pathological ventricular wall thickening, which in turn increases all stress and wall thickening during MI progression (8).

The injection of natural or synthetic hydrogel materials into the ventricular wall has become an excellent therapeutic strategy to break the stress feedback pathway, as it reduces the stress load on the ventricular wall by increasing the thickness of the ventricular wall and reshaping the left ventricular geometry, providing mechanical support to the myocardial area and promoting myocardial tissue repair (9-13). A clinical trial of alginate-hydrogel injection treatment was shown to have a good therapeutic effect and the therapeutic potential to inhibit the damage process after MI, and the safety of hydrogel materials injection has also been validated in several clinical trials (14-18).

It has been reported that the matrix hardness of myocardial cells adjacent to the hydrogel material changes after the hydrogel is injected into the ventricular wall (19-21). However, matrix hardness has been shown to alter various cellular behaviors (22-26), including the inflammatory phenotypes of various cells (27-29). Thus, we sought to analyze transcriptomic changes three days after the injection of alginate hydrogel into the infarcted ventricular wall following the early inflammatory response of MI to identify transcriptomes for a possible novel mechanism for cardiac function improvement. Differentially expressed genes (DEGs) were screened using the following criteria: $P<0.05$, and log-fold change >1.5. An enrichment analysis of the Gene Ontology (GO; http://www.geneontology.org) and Kyoto Encyclopedia of Genes and Genomes (KEGG; http://www.genome.jp/kegg) databases was performed using KOBAS 3.0. We also built a protein-protein interaction (PPI) network using the Search Tool for the Retrieval of Interacting Genes/Proteins (STRING) database (https://string-db.org/) and the Cytohubba plug-in

<div style="border:1px solid #ccc; padding:8px;">

Highlight box

Key findings
- Our findings suggest that the injectable hydrogel directly alters the inflammatory response and the chemokine-mediated signaling pathway of cardiomyocytes, ultimately improving cardiac function.

What is known and what is new?
- As an injectable biomaterial, alginate hydrogel can provide mechanical support to the myocardial infarction (MI) and is mostly used as a carrier for the delivery of targeted drugs, which has achieved exciting results in clinical trials.
- There are few reports on whether hydrogels on their own can improve heart function, this study sought to explore these mechanisms in an animal model of MI.

What is the implication, and what should change now?
- This study provides strong evidence that beta-2-microglobulin (*B2m*) contributes to the development of MI by influencing early inflammation or oxidative stress after MI, and the mechanism of *B2m* expression change in response to hydrogel therapy requires further study.

</div>

in Cytoscape. By extracting and analyzing a cluster module in the PPI network, we identified 10 central genes related to chemokines and the immune response. Finally, beta-2-microglobulin (*B2m*) was identified as a potential alginate-hydrogel response gene through a literature search and validation in cell experiments. In addition, by combining the analysis with the Molecular Signatures Database (MSigDB; https://www.gsea-msigdb.org/gsea/msigdb), we obtained additional genes that may be involved in alginate-hydrogel therapy to improve cardiac function by influencing hypoxic stimulation and the inflammatory response. This study provides new insights into the mechanism by which alginate hydrogel alleviates myocardial dysfunction in MI by influencing the inflammatory response at the transcriptome level. We present this article in accordance with the ARRIVE reporting checklist (available at https://jtd.amegroups.com/article/view/10.21037/jtd-24-358/rc).

Methods

Study design

An MI model will be established in male C57BL/6J mice by ligation of the proximal left anterior descending (LAD) coronary artery, the flow diagram was illustrated in *Figure 1A*. Following the induction of MI, the mice will be randomly assigned to four groups: (I) sham (chest incision and closure but no coronary ligation); (II) MI only (coronary ligation without any injection); (III) MI with saline injection [coronary ligation with local injection of saline (volume and timing similar to hydrogel)]; (IV) MI with hydrogel injection (coronary ligation with local injection of saline). The specific method for grouping can be found in the supplemental file (Appendix 1). Four weeks post-MI, RNA will be isolated from the infarcted hearts of mice. Subsequently, RNA sequencing will be performed to identify differentially expressed messenger RNAs (mRNAs) between the saline group and the hydrogel group. The identified mRNAs will then undergo comprehensive analysis using GO and KEGG pathway analysis to elucidate the biological processes and molecular pathways associated with the differential gene expression.

Animals

The 8-week-old male C57BL/6J mice (25±2 g, n=46) were purchased from the Guangdong Medical Experimental Animal Center (Guangzhou, China) and domesticated in the specific pathogen free laboratory for three days before the experiment. The mice were raised under standard conditions of humidity (50%±10% relative humidity) and temperature (20±2 ℃) on a 12-hour dark/light cycle, and were provided with food and water ad libitum. The animal experiments were conducted in accordance with the Guide for the Care and Use of Laboratory Animals, 8th edition. This study was approved by the Ethics Review Committee of The First Affiliated Hospital of Guangzhou Medical University (No. 2022365). A protocol was prepared before the study without registration.

Left ventricular infarction and intramyocardial injection model

In brief, the mice were anesthetized via isoflurane (2.0%) inhalation with oxygen (100%) and placed on a warm operating plate. The mice were then intubated and placed on respiratory support with a rodent volume-controlled mechanical ventilator (RWD Life Science Co. Ltd., Guangzhou, China). The mice were fixed in the supine position, and the chest was shaved and prepared with povidone-iodine solution. Left ventricular infarction was induced by ligation of the proximal LAD with 7-0 absorbable polypropylene sutures at approximately 3 mm below the left atrial appendix, as described previously (30). After 30 minutes from LAD ligation, intramyocardial injections (hydrogel or saline according to the experimental group) were performed in the proximal wall regions bordering the infarct area, as well as the center of the infarct area (with one 20-μL injection). The opened intercostal incision was closed manually, and the skin was then closed in layers with 5-0 polypropylene skin sutures. The sham group had the intercostal space incised and sutured without receiving neither the LAD ligation nor the injections. The MI only had LAD ligation but no myocardial injection. The mice were returned to their cages after recovering from the anesthesia.

Before fabricating the hydrogels, sodium alginate and sodium alginate were completely dissolved in H_2O to form 0.5–5.0 wt% and 1.0–5.0 wt% solutions, respectively, at 25 ℃. The hydrogels were prepared rapidly at 25 ℃ at a volume ratio of 7:9–9:7, and then drawn into a sterile syringe and mixed, after which, they were equilibrated at 25 ℃ for 20–50 minutes to form a stable hydrogel. The final concentrations of Na^+ were 140–160 mmol/L, respectively.

2446

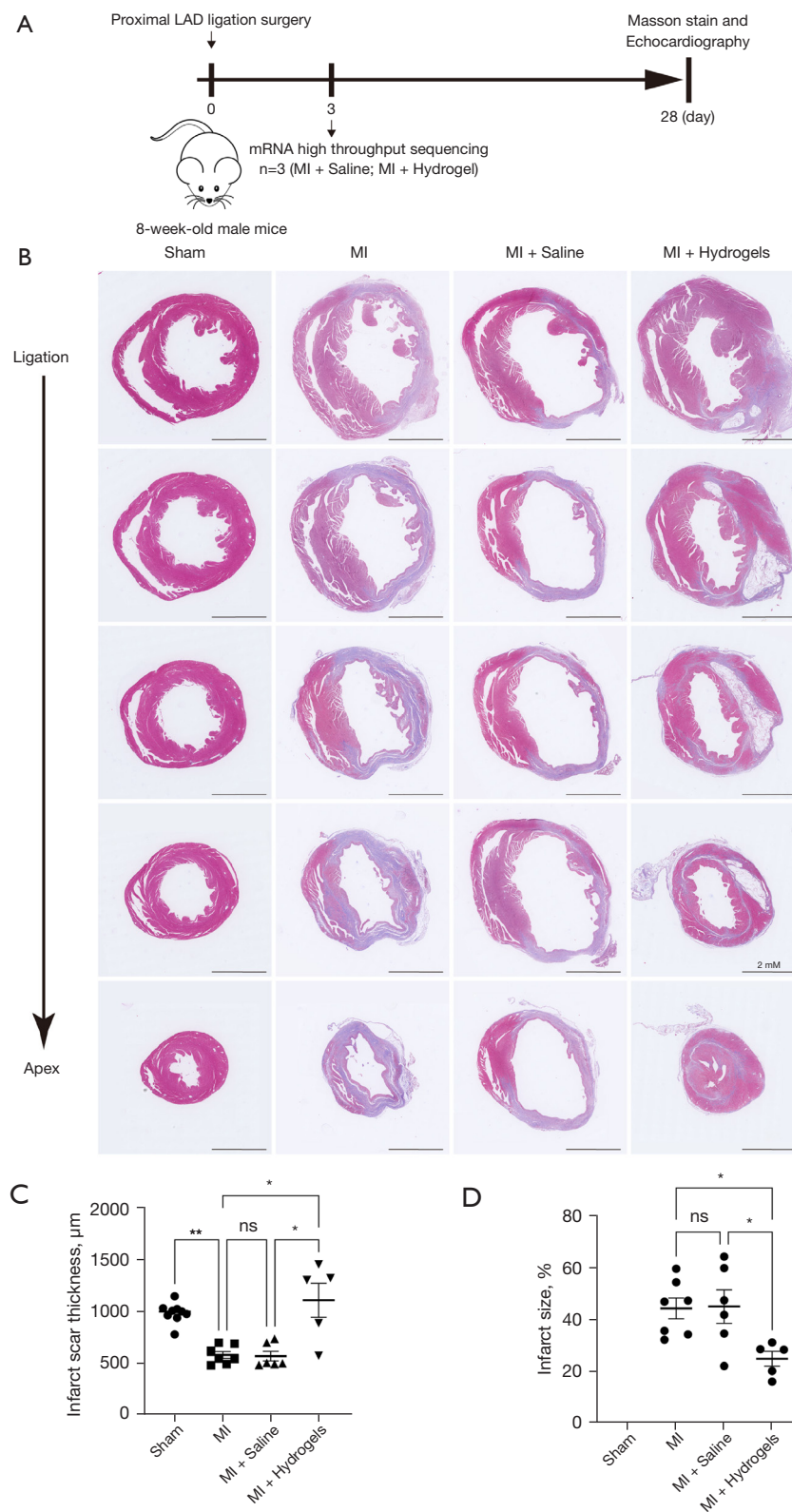Wang et al. Transcriptome analysis of hydrogel treatment for MI

Figure 1 Histological changes after myocardial infarction. (A) A flow diagram of animal experiment and operations time. (B) Masson trichrome staining (scale: 2 mM). Quantitative analysis of infarct wall thickness (C) and infarct area (D) after 28 days of alginate-hydrogel

injection treatments. *, P<0.05; **, P<0.01; ns, no significance (mean ± SEM, n≥5). When comparing the infarct wall thickness and infarct area for each group, we count the average of five slices for each sample. All experimental mice were divided into four groups: sham, sham operation group; MI, myocardial invasion operation group; MI + saline, intrinsic injection of sterile 0.9% sodium chloride solution after myocardial invasion surgery; MI + hydrogels, intrinsic injection of estimate hydraulic after myocardial invasion surgery. The slice numbers for the four groups used for analysis were sham 1–9, MI 1–7, MI + saline 1–6 and MI + hydrogels 1–5. LAD, left anterior descending; mRNA, messenger RNA; MI, myocardial infarction; SEM, standard error of the mean.

Echocardiography

The mice were anesthetized with isoflurane inhalation with 100% oxygen. After 28 days of treatment, standard transthoracic echocardiography studies were performed using the using a Vevo2100 ultra-high frequency ultrasound imaging system (Fujifilm Visualsonics, Inc., Toronto, Ontario, Canada) in a phased array format. B-mode measurements were performed on the left ventricular short axis view (at the papillary muscle level). The end-diastolic area (EDA) and end-systolic area (ESA) left ventricular lumen areas and diameters were measured by tracking the endocardium boundary. The M-mode tracking image was also recorded from the same short axis view, and left ventricular end-systolic diameter (LVESD) and left ventricular end-diastolic diameter (LVEDD) were measured. Left ventricular end-systolic volume (LVESV) and left ventricular end-diastolic volume (LVEDV) were estimated according to the diameters. The left ventricular-ejection fraction (LVEF) and left ventricular-fractional shortening (LVFS) percentages of the left ventricle were automatically calculated by an Echometer. Echocardiographic measurements were averaged from at least three separate cardiac cycles. The operators, who conducted the echocardiography examinations and took the image measurements, were blinded to the animal treatment assignment.

Histological analysis and fluorescence immunohistochemistry assay

The mice were euthanized after being anesthetized, and then their hearts were exposed. A tear was created at the right atrial appendage with scissors, and 5 mL of low-temperature sterile phosphate-buffered saline (PBS) buffer and 4% cold paraformaldehyde were slowly infused near the apex of the left ventricle. The heart was removed and fixed in 4% paraformaldehyde at 4 ℃ for 12 hours. The paraformaldehyde-fixed mouse myocardium specimens were embedded in paraffin and cut into 4 µm thick sections. The tissue sections were stained with Masson's trichrome for the histological analyses. To analyze the collagen volume fraction (CVF) in the border zone of the infarcted region, we selected five separate views (magnification = original ×400) and assessed the CVF using the following formula: CVF = collagen area/total area. For the immunohistochemistry analyses, each piece of heart was sealed with 10% goat serum in PBS as blocking buffer at room temperature for one hour, and an anti-*B2m* rabbit polyclonal antibody (1:500, ProteinTech Group, Chicago, Illinois, USA) was used. The nucleus was stained with 2-(4-amidinophenyl)-6-indolecarbamidine dihydrochloride [antifade mounting medium with DAPI (4',6-diamidino-2-phenylindole), Beyotime Biotechnology, Shanghai, China]. The NanoZoomer S360 was used to inspect the general pathological slide and images were captured using NDP. view2 viewing software (Hamamatsu Photonics K.K., Shimokanzo, Shizuoka Ken, Japan). Pannoramic SCAN II was used to inspect the fluorescent slides and images were captured using CaseViewer software (3DHISTECH Ltd., Budapest, Hungary). ImageJ was used for all the measurements and evaluations. For each recovered sample, five different photographs were taken under the microscope field of view at a magnification of 100 times.

Measuring the infarct area, scar area, and left ventricular anterior wall thickening

After Masson trichrome staining, a digital image was captured of the cross-sectional plane. The infarct size was defined as the percentage of the sum of epicardium and endocardium infarct perimeter divided by the sum of left ventricular epicardium and endocardium infarct perimeter. The thickness of the left ventricular anterior wall was expressed as follows: scar area/[(epicardial perimeter + endocardium perimeter)/2]. Each parameter was measured (n=6 per group) using ImageJ.

Library construction and mRNA sequencing

To obtain high-quality RNA for sequencing (from the

2448

Wang et al. Transcriptome analysis of hydrogel treatment for MI

day-three hearts in particular), the left ventricular infarction area was cut from the hearts of the MI only group mice, and the same area was cut from the hearts of the sham group mice to obtain three biological replicates. RNA was isolated separately for each biological replicate from the MI area of the left ventricular infarction area of the mice and the corresponding site in the sham group using Trizol Reagent (Megan, Guangzhou, Guangdong, China) according to the manufacturer's instructions. RNA purity was assessed using the Nanodrop 3300 Spectrophotometer (ThermoFisher Scientific, Waltham, Massachusetts, USA), and the integrity was evaluated using the Agilent 2200 TapeStation System (Agilent Technologies, Palo Alto, California, USA), and only samples with RNA integrity numbers >7.0 the analysis were included.

The total RNA was fragmented to approximately 200 bp. In accordance with the instructions of the NEBNext Ultra RNA Library Prep Kit for Illumina (New England Biolabs, Ipswich, Massachusetts, USA), the fragmented RNA was subsequently subjected to first and second strand complementary DNA (cDNA) synthesis, followed by adaptor ligation and enrichment using a low number of cycles. The purified library products were accessed using the Agilent 2200 TapeStation and Qubit 2.0 (Life Technologies, Carlsbad, California, USA). The libraries were then paired-end sequenced (PE150) using the Illumina HiSeq 3000 platform (RiboBio, Guangzhou, China).

Optimization of the sequencing data/quality control

Raw FASTQ sequences were processed using the flexible read trimming tool Trimmomatic (v.0.36). After removing the trailing fractions with Phred quality scores under 20 and uniform sequence lengths, the remaining sequences underwent the downstream clustering process. FastQC software was used for the quality control analysis of the sequenced reads. The adapter removal, trimming, identification, and read merging were performed using Trimmomatic. Reads with a shear base quality under Q20 as determined by the sequencing were cut from the end, until their sequences were under 25 bp.

Quantification of gene expression levels

The paired-end reads were compared with the house mouse reference genome GRCm38 using HisAT2 software. The Python library HTSeq was used to calculate the read numbers for each gene. The overall gene expression levels of each sample were displayed as the expected number of reads per kilobase of transcript sequence per million base pairs sequenced.

Differential expression analysis

Using DEGseq software, the statistically significant DEGs were those that had adjusted P value thresholds <0.05 and $|\log_2(\text{fold change})| > 1$.

RNA extraction and quantitative reverse transcriptase polymerase chain reaction (qRT-PCR)

RNA was extracted separately for each biological replicate from the MI area of left ventricular samples using Trizol Reagent (Megan Biotech, Guangzhou, China) in accordance with the manufacturer's instructions. The concentration and quality of the total RNA samples were measured using the NanoDrop 3300 Spectrophotometer (ThermoFisher Scientific). RNA integrity was assessed by electrophoresis using denaturing agarose gels. High-quality RNA samples were used to synthesize the cDNA via the HiScript® III 1st Strand cDNA Synthesis Kit (+ gDNA wiper) (Vazyme, Nanjing, Jiangsu, China) in accordance with the manufacturer's protocol. Finally, the qRT-PCR was performed using the SYBR® Green Premix Pro Taq HS Kit (Accurate Biology, Changsha, Hunan, China) with gene-specific primers in a Bio-Rad CFX96 system (Bio-Rad, Hercules, California, USA). RNA relative expression levels were calculated using the $2^{-\Delta\Delta CT}$ method against the internal control glyceraldehyde-3-phosphate dehydrogenase.

GO terms and KEGG pathway enrichment analysis

All the differentially expressed mRNAs were analyzed by a GO and KEGG pathway analysis. The GO analysis was performed using KOBAS 3.0 software. GO, and all the differentially expressed transcripts were classified according to their gene function and transcription attributes, which included the molecular function, cellular component, and biological process. In addition, KEGG KOBAS 3.0 software was used to analyze the differentially expressed mRNAs with respect to the enrichment of different pathways.

PPI network

PPI pairs for *B2m* were predicted using the STRING database (https://version-11-0.string-db.org/). The PPI

network was constructed by a protein chip technology with a confidence level ≥0.9 and was visualized using Cytoscape software. The Cytoscape plug-in CytoHubba was used to find the key genes in the PPI network Five methods in the CytoHubba plug-in were combined to identify the hub genes, including the edge percolation component (EPC), maximal clique centrality (MCC) (leading edge centrality), maximum neighbor component (MNC), degree (node connectivity), and closeness (node connectivity tightness). A thorough analysis of all the data led to results, which were then used to identify the key genes associated with the immune system.

Cell culture and transfection

HL-1 cells were purchased from Immocell (Immocell Biotechnology Co., Ltd., Xiamen, China) and were cultured in high sugar medium Dulbecco's modified eagle medium (DMEM) supplemented with 10% fetal bovine serum, 2 mM of glutamine, 100 U/mL of penicillin, 0.1 mg/mL of streptomycin, 50 μg/mL of gentamicin, and 1 mM of pyruvate in a humidified air incubator containing 5% carbon dioxide (CO_2) at 37 ℃. For the hypoxia injury models, the cells were pre-incubated in serum-free and glucose-free DMEM medium for 24 hours, and the HL-1 cells were subsequently cultured in a hypoxia chamber with 5% CO_2 and 95% N_2 for 12 hours at 37 ℃. The hydrogel pre-coated plate served as the treatment group (0.2 g/mL).

Western blot

For the western blot analysis, the cells were washed with cold PBS and lysed in ice-cold RIPA solution (EpiZyme, Shanghai, China) containing proteinase inhibitor (Invitrogen, Carlsbad, California, USA) to obtain the lysis solution. The supernatants and Multicolor Prestained Protein Ladder molecular mass marker (EpiZyme, Shanghai, China) were electrophoresed using the 10% PAGE Gel Fast Preparation Kit and transferred onto Immobilon®-NC transfer membranes (Merck Millipore, Darmstadt, Hessen, Germany). The membranes were blocked with protein-free rapid blocking buffer (EpiZyme, Shanghai, China), and an anti-*B2m* rabbit polyclonal antibody (1:1,000, ProteinTech Group, Chicago, Illinois, USA) was used to examine the protein expression level of *B2m*. Protein expression was detected with the Omni-ECL™ Femto Light Chemiluminescence Kit (EpiZyme, Shanghai, China).

Statistical analysis

The statistical analysis was conducted using GraphPad Prism 9 (GraphPad Software) and SPSS 25.0 (IBM Corp., Armonk, NY, USA). The data are presented as the mean ± standard error of the mean (SEM). The Student's *t*-test for unpaired observations was used to analyze the differences between the two groups. To assess the short-term effects of MI on cardiac function, a one-way repeated measures analysis of variance (ANOVA) was conducted, after which the Bonferroni test was used to examine specific differences. A single-factor ANOVA and the Tukey test were used for all the multi-group comparisons in the study. A P value <0.05 was considered statistically significant.

Results

Injectable alginate hydrogels improve cardiac function after MI

At 28 days, scar tissue rich in collagen was found in all MI groups (MI only, saline injection, and hydrogel injection groups) (*Figure 1B*). The remaining hydrogel material was surrounded by tissues that reacted with the foreign body. In terms of wall thickness, the hydrogel injection significantly improved the decrease in wall thickness 4 weeks after MI. Compared with the MI control group, the infarct size of the hydrogel group was also significantly reduced (*Figure 1C,1D*). Conversely, the group undergoing intramyocardial injection of saline did not maintain the left ventricular wall thickness or limit the infarct size, compared to the MI only group.

At 56 days after MI, echocardiographic cardiac function was decreased in MI groups compared to sham animals (*Figure 2*). However, the hydrogel group presented significantly better left ventricular indexes for all measured parameters (LVEF, LVFS, LVESV, LVEDV, LVESD, and LVEDD), when compared to other MI groups (MI only and MI + saline).

Expression profile of mRNAs in hearts with acute MI

To identify the differentially expressed mRNAs between the saline group and the hydrogel treatment group, we analyzed the total RNA sequences isolated from the infarcted area using DEGSeq software. The mRNA differential expression profiles in the heart samples from the saline group and hydrogel treatment group were used to generate a volcano map, which showed the expression profiles of all the mRNAs (*Figure 3A*). Differential expression transcripts
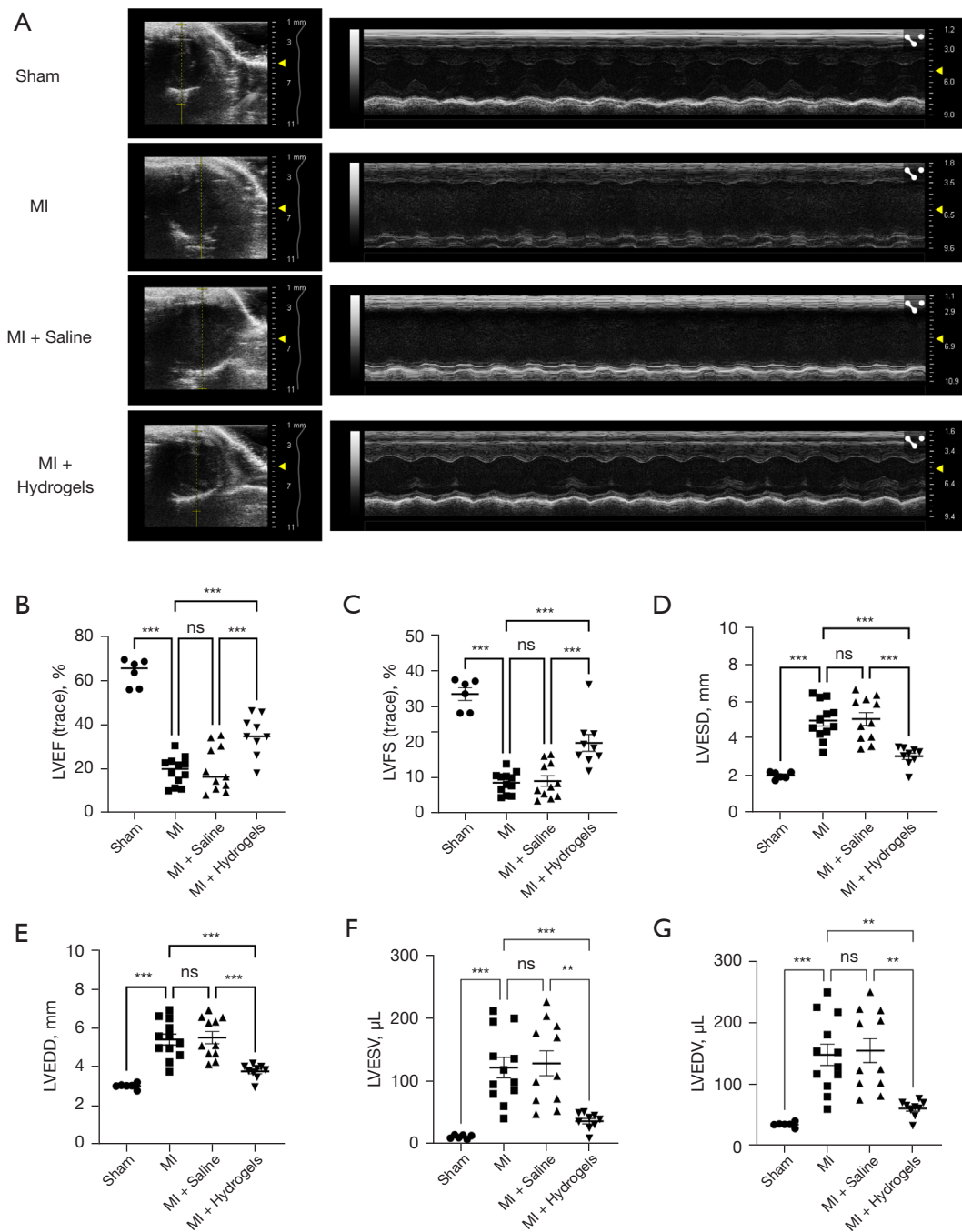
2450

Wang et al. Transcriptome analysis of hydrogel treatment for MI

Figure 2 Changes in cardiac function after myocardial infarction. After 28 days of treatment, cardiac function indicators were measured by echocardiography, including echocardiography images and related LVEF, LVFS, LVESD, LVEDD, LVESV, and LVEDV analyses (A-G). **, $P<0.01$; ***, $P<0.001$; ns, no significance (mean ± SEM, n≥6). All experimental mice were divided into four groups: sham; MI; MI + saline and MI + hydrogels, as mentioned before. MI, myocardial infarction; LVEF, left ventricular-ejection fraction; LVFS, left ventricular-fractional shortening; LVESV, left ventricular end-systolic volume; LVEDV, left ventricular end-diastolic volume; LVESD, left ventricular end-systolic diameter; LVEDD, left ventricular end-diastolic diameter; SEM, standard error of the mean.
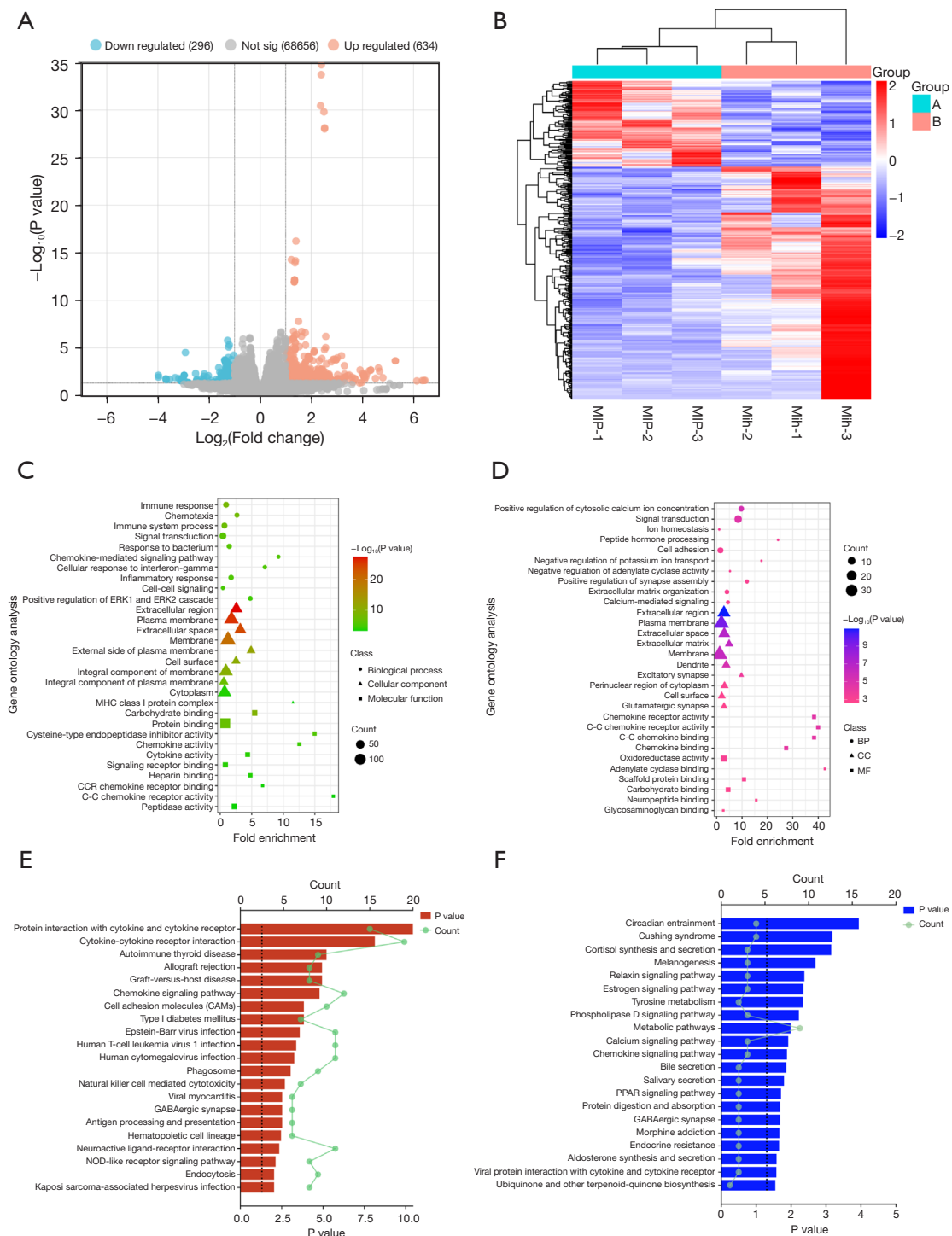
Figure 3 The expression profiles, hierarchical clustering heatmaps, GO and KEGG pathway analysis results of the differentially expressed mRNAs. (A) Volcano plot of gene expression. The red dots represent upregulated expression, and the blue dots represent downregulated expression (fold change ≥2.0, P<0.05, two-tailed *t*-test), while the gray dots indicate no difference. (B) Hierarchically clustered heatmap of differentially expressed mRNAs (P<0.05). Group A, the hydrogel treatment group; group B, the saline group. The top 10 enrichment score values for the GO enrichment terms related to statistically significant (C) upregulated mRNAs, and (D) downregulated mRNAs. The top 20 pathways based on the statistically significant (E) upregulated mRNAs, and (F) downregulated mRNAs. BP, biological process; CC, cellular component; MF, molecular function; GO, Gene Ontology; KEGG, Kyoto Encyclopedia of Genes and Genomes; mRNA, messenger RNA.

Table 1 The top 30 differentially expressed mRNAs

Gene	Length	Chromosome	Regulation	log$_2$(fold change)	P value
Alox12e	2,374	11	Down	−3.982219	0.007
Mzf1	2,975	7	Down	−3.981066	0.01
Clec18a	2,289	8	Down	−3.694272	0.01
Zfp966	1,811	2	Down	−3.674667	0.01
Pcare	5,055	17	Down	−3.674423	0.02
Wnt7a	3,007	6	Down	−3.540929	0.02
Reg3a	837	6	Down	−3.323078	0.01
Ptprt	12,159	2	Down	−3.098134	0.02
Otogl	9,009	10	Down	−2.971874	0.007
Frmpd1	4,827	4	Down	−2.970306	0.03
Clec3a	2,930	8	Down	−2.923488	3.03E−05
E230025N22Rik	1,674	18	Down	−2.893691	0.03
Lrrtm2	5,673	18	Down	−2.809323	0.04
Duoxa1	1,478	2	Down	−2.805577	0.04
Cdhr4	2,517	9	Down	−2.524543	0.005
Folh1	3,047	7	Up	6.445573	0.02
Ubd	947	17	Up	6.124339	0.02
Enthd1	2,929	15	Up	5.286715	<0.001
Aldh3b2	2,161	19	Up	4.799055	0.01
Tmem45b	1,602	9	Up	4.668139	0.002
C130026I21Rik	1,883	1	Up	4.624015	0.001
H2-M9	1,122	17	Up	4.51129	0.01
Cst9	687	2	Up	4.15195	0.006
Ear1	739	14	Up	4.128527	0.01
Rhcg	1,650	7	Up	4.068424	0.01
Adrb3	2,942	8	Up	4.051393	0.009
C6	1,667	15	Up	4.046177	0.008
Tshr	4,332	12	Up	3.998236	0.005
Gpr158	7,143	2	Up	3.961846	0.04
Cxcl13	1,162	5	Up	3.907923	0.002

mRNA, messenger RNA.

were defined as |log$_2$(fold change)| >1.

We found that compared with hydrogel treatment group, 250 mRNAs were upregulated and 92 mRNAs were downregulated in saline group (P<0.05). The top 30 differentially expressed mRNAs were listed (*Table 1*).

According to the cluster-analysis heat map, there were significant differences in the mRNA expression patterns between the saline group and the hydrogel treatment group (*Figure 3B*). This difference indicates that the injection of alginate hydrogel into the left ventricular wall after MI

improved cardiac function in mice following the infarction, while also significantly changed mRNA expression.

GO and KEGG pathway analysis

A GO enrichment analysis was conducted to screen the differentially expressed mRNAs, which included those that were upregulated (*Figure 3C*) and those that were downregulated in saline group (*Figure 3D*). The upregulated mRNAs were mostly related to the immune response, chemokine-mediated signaling pathway, and inflammatory response, while the downregulated mRNAs were mostly associated with signal transduction, chemokine-receptor activity, C-C chemokine-receptor activity, C-C chemokine binding, and chemokine binding. The KEGG pathway analysis revealed that the upregulated mRNAs mainly participated in the pathways associated with the cytokine-cytokine receptor interaction, chemokine-mediated signaling pathway, and NOD-like receptor signaling pathway (*Figure 3E*), while the downregulated mRNAs mainly corresponded to the pathways associated with the metabolic pathways, the chemokine-mediated signaling pathway, and the PPAR signaling pathway (*Figure 3F*).

To reduce the number of candidate mRNAs potentially involved in the hydrogel treatment, using the GO term enrichment analysis, we first selected the mRNAs that were associated with the MI-related protein-coding genes. After the functional annotation and enrichment analysis, we found: (I) 22 protein-coding genes [*B2m*; C-C motif chemokine ligand 2 (*Ccl2*); interleukin 10 (*Il10*); C-C motif chemokine receptor 10 (*Ccr10*); interleukin 7 (*Il7*); histocompatibility 2, M region locus 9 (*H2-M9*); T cell specific GTPase 2 (*Tgtp2*); atypical chemokine receptor 4 (*Ackr4*); interferon induced protein 44 (*Ifi44*); secretory leukocyte peptidase inhibitor (*Slpi*); C-C motif chemokine ligand 6 (*Ccl6*); C-C motif chemokine ligand 7 (*Ccl7*); C-C motif chemokine ligand 5 (*Ccl5*); histocompatibility 2, Q region locus 4 (*H2-Q4*); histocompatibility 2, Q region locus 7 (*H2-Q7*); histocompatibility 2, Q region locus 6 (*H2-Q6*); C-C motif chemokine receptor 1 (*Ccr1*); C-C motif chemokine receptor 3 (*Ccr3*); C-X-C motif chemokine receptor 1 (*Cxcr1*); C-X-C motif chemokine ligand 13 (*Cxcl13*); myelin basic protein (*Mbp*); C-X-C motif chemokine ligand 9 (*Cxcl9*)] that were associated with the immune response; (II) eight genes [*Ccl2*, *Ccl6*, *Ccl7*, *Ccl5*, *Cxcl9*, C-C motif chemokine ligand 17 (*Ccl17*), *Ccr1*, and *Cxcl13*] that were related to the chemokine-mediated signaling pathway; (III) 22 genes [*H2-Q7*; *B2m*; guanylate

binding protein 2b (*Gbp2b*); secretory leukocyte peptidase inhibitor (*Slpi*); ficolin A (*Fcna*); CD19 molecule (*Cd19*); macrophage receptor with collagenous structure (*Marco*); interferon regulatory factor 7 (*Irf7*); Z-DNA binding protein 1 (*Zbp1*); T cell-interacting, activating receptor on myeloid cells 1 (*Tarm1*); CD300 molecule like family member f (*Cd300lf*); SLAM family member 7 (*Slamf7*); complement C2 (*C2*); signaling lymphocytic activation molecule family member 1 (*Slamf1*); protein tyrosine phosphatase non-receptor type 22 (*Ptpn22*); interleukin 2 receptor subunit alpha (*Il2ra*); Fc mu receptor (*Fcmr*); TNF receptor superfamily member 13C (*Tnfrsf13c*); complement factor B (*Cfb*); serine (or cysteine) peptidase inhibitor, clade A, member 3G (*Serpina3g*); CD3 epsilon subunit of T-cell receptor complex (*Cd3e*); CD5 molecule like (*Cd5l*)] that were correlated with the inflammatory response; (IV) 12 genes [A-kinase anchoring protein 5 (*Akap5*); SHC adaptor protein 3 (*Shc3*); atypical chemokine receptor 4 (*Ackr4*); C-C motif chemokine receptor 10 (*Ccr10*); cholinergic receptor nicotinic alpha 10 (*Chrna10*); galanin receptor 2 (*Galr2*); somatostatin receptor 3 (*Sstr3*); C-C motif chemokine receptor 3 (*Ccr3*); FERM and PDZ domain containing 1 (*Frmpd1*); t-complex 11 (*Tcp11*); diacylglycerol kinase beta (*Dgkb*); Wnt family member 7A (*Wnt7a*)] that were associated with signal transduction; (V) three gene (*Ackr4*, *Ccr10*, and *Ccr3*) that were associated with chemokine-receptor activity; and (VI) three genes (*Ackr4*, *Ccr10*, and *Ccr3*) that were associated with chemokine binding.

PPI network construction

The PPI network generated by the STRING database revealed an interaction between two proteins encoded by the DEGs (*Figure 4A*). Using the CytoHubba plug-in to determine the importance of genes in the genome, we identified eight immune system-related hub genes using at least five cell beam target prediction tools. These genes scored highly across the five target prediction techniques for the cell walls and were critical to understanding the pathogenesis of MI (*Figure 4B*).

Verification of mRNA expression using qRT-PCR

Based on our differentially expressed mRNA profiles, we randomly chose 10 mRNAs for qRT-PCR validation, of which, three were upregulated (*B2m*, *Chil3*, and *Adamtsl*) and three were downregulated (*Ccl6*). The results were in line with the expression trends detected by the high-
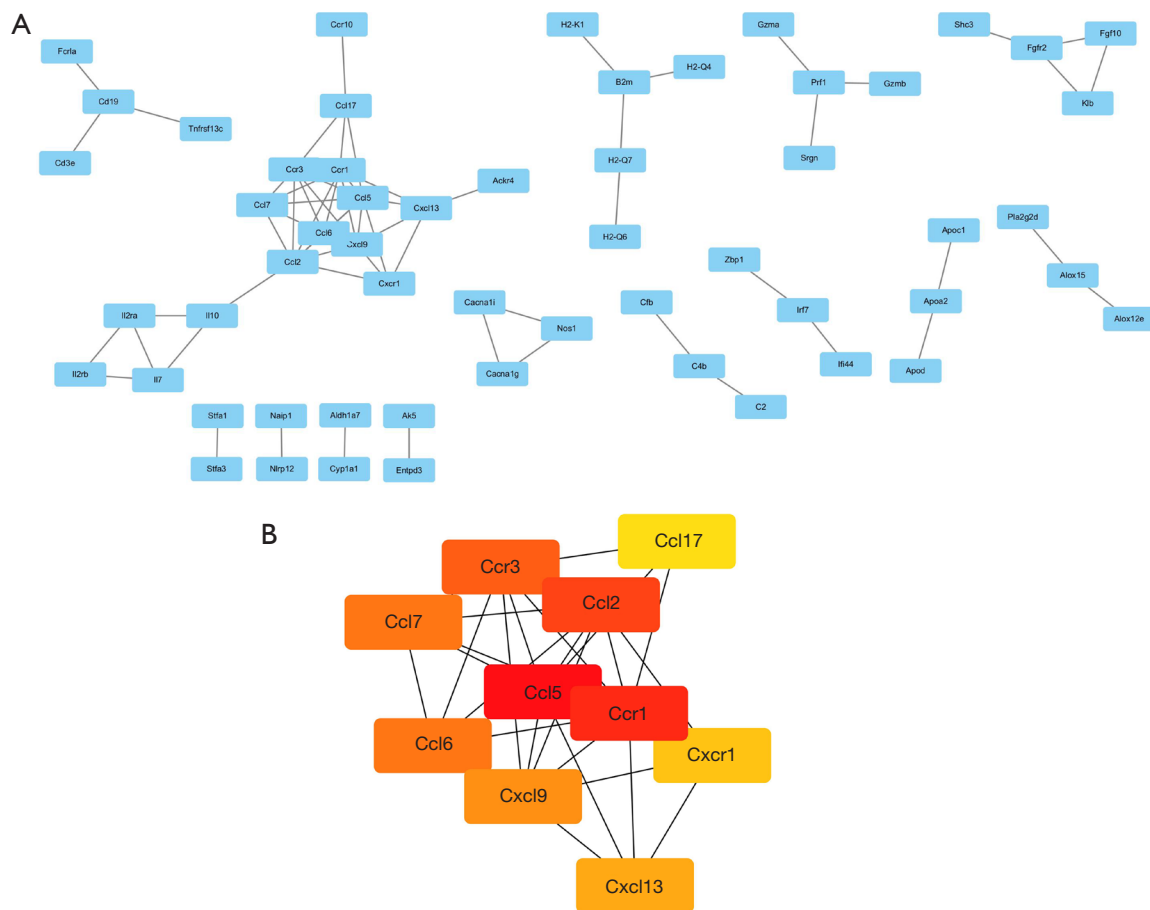
2454

Wang et al. Transcriptome analysis of hydrogel treatment for MI

Figure 4 The PPI network. CytoHubba revealed a DEG PPI network with one cluster component. (A) The PPI network generated by the DEGs. The relationships between the proteins are represented by nodes and edges in the graph. (B) CytoHubba was used to extract a cluster module. PPI, protein-protein interaction; DEGs, differentially expressed genes.

throughput sequencing (*Figure 5A,5B*).

Hydrogel reversed the upregulation of B2m induced by OGD

B2m, a major histocompatibility complex class I molecule, plays a key role in antigen presentation and processing, inflammation, and the oxidative stress response (31,32). In our study, *B2m* was identified as a key gene in response to the alginate-hydrogel improvement of cardiac function in MI. Thus, we subjected cultured mouse HL-1 cardiomyocytes to oxygen and glucose deprivation (OGD) and established a hypoxic-ischemic injury in the MI model. Alginate hydrogel was also used as the cell-

adhesion substrate to explore the protective effect of alginate hydrogel on decreased cardiac function after MI. The expression of *B2m* was significantly upregulated in the saline group, and the hydrogel substrate inhibited the upregulation of *B2m* induced by OGD (*Figure 5C*). We evaluated the expression of *B2m* in the OGD HL-1 cells by western blotting. Qualitatively, compared with the control group, the expression of *B2m* in the OGD group was significantly upregulated, and the hydrogel substrate inhibited the upregulation of *B2m* induced by OGD ($P<0.05$) (*Figure 5D*). These data clearly indicate that the mechanism by which alginate hydrogel improves cardiac function and reduces cardiac remodeling ability may be related to changes in *B2m* expression.
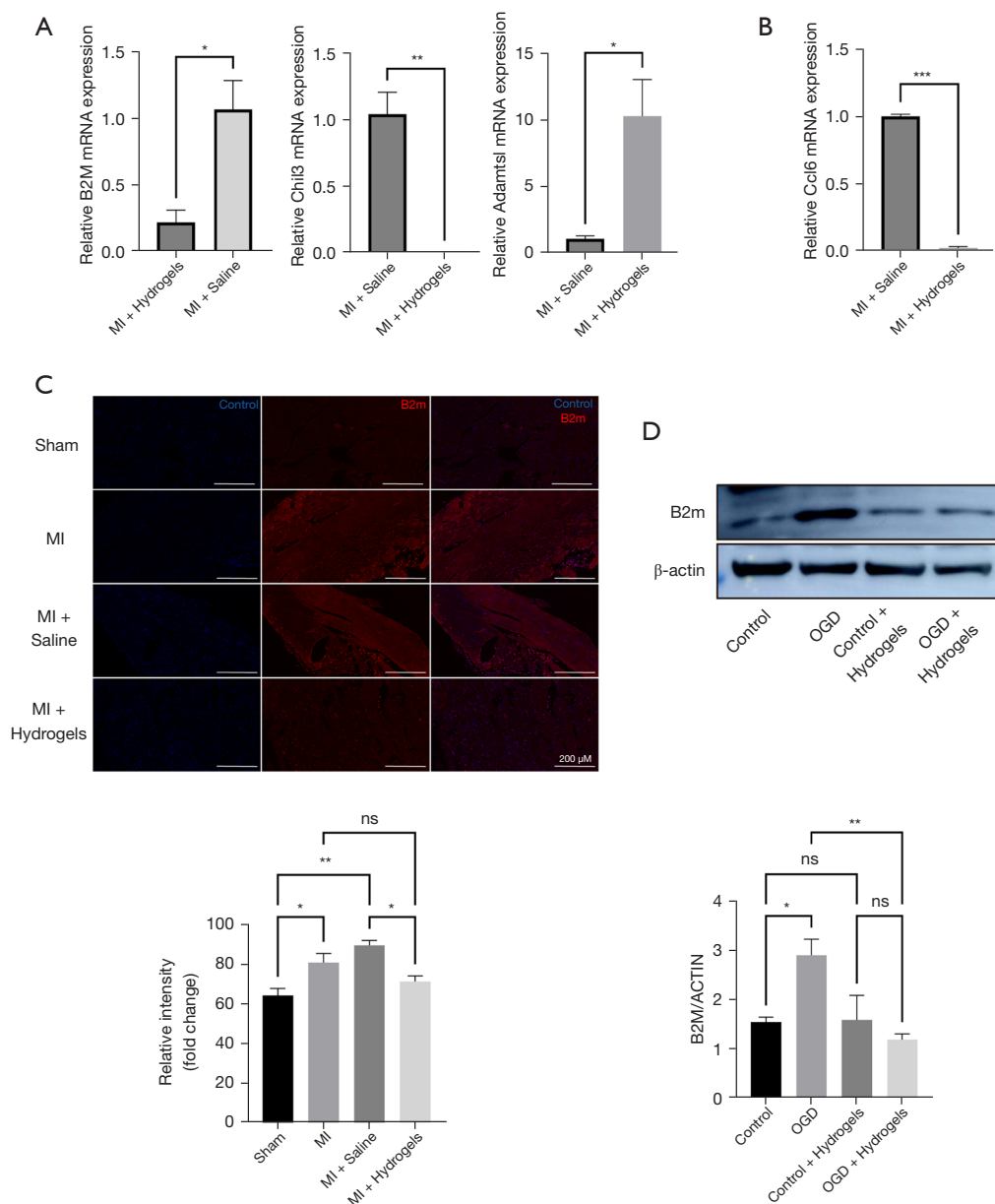
Figure 5 qRT-PCR verification for selected differentially expressed mRNAs. Validation for (A) upregulated mRNAs, and (B) downregulated mRNAs by qRT-PCR (n=3 in each group; the significance was assessed by an unpaired *t*-test analysis as appropriate). (C) Immunofluorescence staining of tissues. The B2m expression of the infarcted hearts after hydrogel injection treatments for 14 days. When comparing the infarct wall thickness and infarct area for each group, we count the average of 5 slices for each sample. (D) The B2m expression of HL-1 cardiomyocytes after OGD treatments for 12 hours (mean ± standard deviation, n=3). *, P<0.05; **, P<0.01; ***, P<0.001; ns, no significance. All experimental mice were divided into four groups: sham; MI; MI + saline and MI + hydrogels, as mentioned before. All experimental cell were divided into four groups: control, cell cultured with complete DMEM medium in normal chamber; OGD, cell cultured with complete DMEM medium in normal chamber for 12 h; control + hydrogels, cell seeded on hydrogel pre-coated plate and then cultured with complete DMEM medium in normal chamber for 12 h; OGD + hydrogels, cell seeded on hydrogel pre-coated plate and then cultured with HBSS solution in hypoxia chamber for 12 h. The slice numbers for the four groups used for analysis were sham 1–3, MI 1–3, MI + saline 1–3 and MI + hydrogels 1–3. B2m, beta-2 microglobulin; mRNA, messenger RNA; MI, myocardial infarction; OGD, oxygen and glucose deprivation; qRT-PCR, quantitative reverse transcriptase polymerase chain reaction; DMEM, Dulbecco's modified eagle medium; HBSS, Hanks' balanced salt solution.
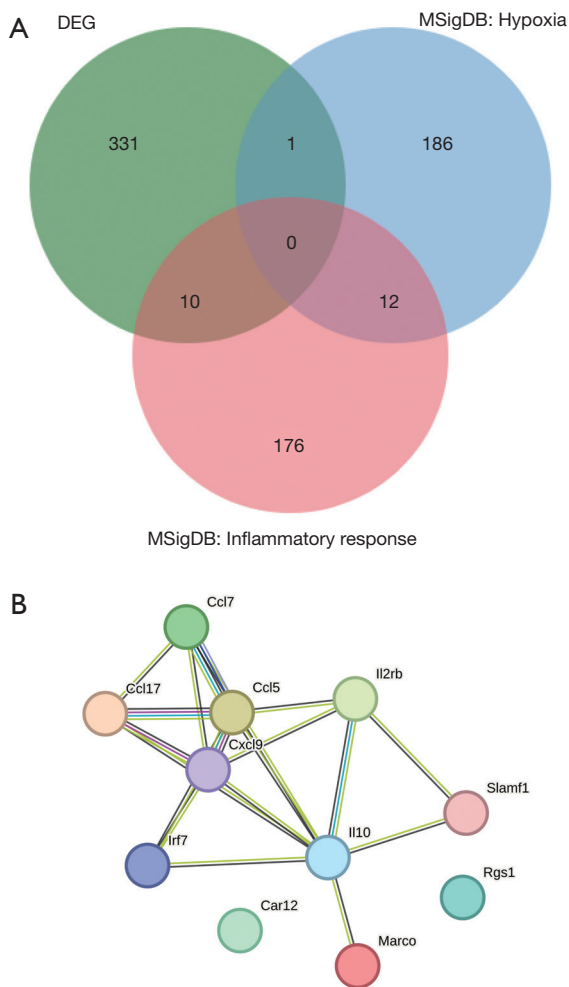
　　　　J Thorac Dis 2024;16(4):2443-2459 | https://dx.doi.org/10.21037/jtd-24-358

2456

Wang et al. Transcriptome analysis of hydrogel treatment for MI

Figure 6 The PPI network. mCODE revealed a DEG PPI network with three cluster components. (A) Venn diagrams of DEGs, MSigDB: (MM3861) hypoxia, and MSigDB: (MM3890) inflammatory response-related gene sets. (B) PPI network generated by hypoxia and inflammatory response-related genes. DEG, differentially expressed gene; MSigDB, Molecular Signatures Database; PPI, protein-protein interaction; mCODE, minimal Common Oncology Data Elements.

Target proteins that may participate in the alginate-hydrogel treatment

MSigDB is a resource of tens of thousands of annotated gene sets, typically used to analyze gene enrichment pathways. To identify the most important genes that may be involved in the reduction of cardiac function after MI following alginate-hydrogel treatment we analyzed common

genes (overlapping genes) between the DEG set and the two known MSigDB data set closely related to MI, inflammatory response (M5932) and hypoxia 447 (M5891) (*Figure 6A*). We found: (I) one protein-coding gene (*Car12*) that was associated with hypoxia (*M5891*); and (II) 10 additional genes (*Marco*, *Irf7*, *Rgs1*, *Cxcl9*, *Slamf1*, *Ccl5*, *Ccl17*, *Il10*, *Ccl7*, and *Il2rb*) that were associated with the inflammatory response (*M5932*), and may play a critical role in alleviating the decline in cardiac function after MI (*Figure 6B*).

Discussion

Intracardiac hydrogel injection has been shown to be a promising therapeutic approach in effectively limiting left ventricular remodeling and functional deterioration. Some injectable therapies are already in clinical trials, but it is important to understand the molecular mechanisms of such therapies to ensure their clinical application are safe and effective.

In this study, we showed that the injection of alginate hydrogel effectively improved cardiac function in mice and alleviated left ventricular remodeling after infarction. This study innovatively performed transcriptome sequencing after alginate-hydrogel injection therapy to fully understand the mechanism of action of alginate hydrogel. The injection of hydrogel materials immediately after MI is not optimal; however, according to previous studies, the injection of hydrogel materials before the reduction of ventricular wall stress may improve cardiac function by affecting mechanisms other than the mechanical action. The transcriptome sequencing results were analyzed through the GO and KEGG signaling pathways and the PPI network, and we found that the injection of alginate hydrogel may exert therapeutic effects on cardiomyocytes during the inflammatory response period after MI by affecting the inflammatory response of cardiomyocytes and the chemokine-related signaling pathways.

We found that *B2m* responded to alginate hydrogel to improve post-MI heart function, with consistent results in the myocyte OGD injury models. *B2m* has been shown to be involved in the inflammation and the pathogenesis of vascular diseases (33,34) and may be an important biomarker in cardiovascular diseases (35,36). In addition, an observational study reported that *B2m* levels were positively associated with cardiovascular disease risk, and this association was independent of traditional cardiovascular disease risk factors and renal function risk factors (37-39).

At present, no studies have clarified the exact relationship

between *B2m* and MI, and the inflammatory response is considered a potential mechanism between *B2m* and cardiovascular diseases (40,41). Another study suggested that *B2m* may play a role in oxidative stress in the elderly, and suggested that *B2m* may serve as a new biomarker of oxidative stress (42). One study suggested that *B2m* is secreted by injured cardiomyocytes and fibrosis via myocardial fibroblasts, thereby participating in cardiac remodeling after ischemic heart injury (43). The mechanism of *B2m* expression change in response to hydrogel therapy requires further study. However, this study provides strong evidence that *B2m* contributes to the development of MI by influencing early inflammation or oxidative stress after MI. In addition, our study identified one and 10 crossover genes, respectively, through a combined analysis of DEGs and the hypoxia and inflammatory response data sets in the MSigDB.

Our next research will focus on conducting animal experiments on whether gene intervention and targeted drug therapy of *B2m* gene expression contributes to the recovery of heart function in mice after MI. In addition, further researches need to be concentrated in exploring the mechanism for regulation of B2M by alginate hydrogel from both physical and biochemical perspectives.

Conclusions

Intramyocardial injection of alginate hydrogel just after closed-artery infarction in mice improved left ventricular function and remodeling. Partial correlation exists between cardiac function improvement by hydrogel injection and *B2m* down-regulation in cardiomyocytes by hydrogel coating. This correlation may be due to the influence of *B2m* on the inflammatory response, chemokine signaling pathways, and oxidative stress during and after infarction.

Acknowledgments

Footnote

Reporting Checklist: The authors have completed the ARRIVE reporting checklist. Available at https://jtd.amegroups.com/article/view/10.21037/jtd-24-358/rc

Data Sharing Statement: Available at https://jtd.amegroups.com/article/view/10.21037/jtd-24-358/dss

Peer Review File: Available at https://jtd.amegroups.com/article/view/10.21037/jtd-24-358/prf

Conflicts of Interest: All authors have completed the ICMJE uniform disclosure form (available at https://jtd.amegroups.com/article/view/10.21037/jtd-24-358/coif). J.Z. is from Hangzhou Deke Medtech Co., Ltd. and Z.C. is from Suzhou NGGT Biotechnology Co., Ltd. The other authors have no conflicts of interest to declare.

Ethical Statement: The authors are accountable for all aspects of the work in ensuring that questions related to the accuracy or integrity of any part of the work are appropriately investigated and resolved. The animal experiments were conducted in accordance with the Guide for the Care and Use of Laboratory Animals, 8th edition. This study was approved by the Ethics Review Committee of The First Affiliated Hospital of Guangzhou Medical University (No. 2022365).

References

1. Zeymer U, Ludman P, Danchin N, et al. Reperfusion therapies and in-hospital outcomes for ST-elevation myocardial infarction in Europe: the ACVC-EAPCI EORP STEMI Registry of the European Society of Cardiology. Eur Heart J 2021;42:4536-49.
2. Wu X, Reboll MR, Korf-Klingebiel M, et al. Angiogenesis after acute myocardial infarction. Cardiovasc Res 2021;117:1257-73.
3. Bostan MM, Stătescu C, Anghel L, et al. Post-Myocardial Infarction Ventricular Remodeling Biomarkers-The Key Link between Pathophysiology and Clinic. Biomolecules 2020;10:1587.
4. Lindsey ML, Brunt KR, Kirk JA, et al. Guidelines for in

2458

Wang et al. Transcriptome analysis of hydrogel treatment for MI

vivo mouse models of myocardial infarction. Am J Physiol Heart Circ Physiol 2021;321:H1056-73.

5. Hage C, Savarese G. Proteomic profiling for investigating the pathophysiology of myocardial infarction. Eur J Prev Cardiol 2023;30:581-2.

6. Saito Y, Oyama K, Tsujita K, et al. Treatment strategies of acute myocardial infarction: updates on revascularization, pharmacological therapy, and beyond. J Cardiol 2023;81:168-78.

7. Bahit MC, Kochar A, Granger CB. Post-Myocardial Infarction Heart Failure. JACC Heart Fail 2018;6:179-86.

8. Del Buono MG, Moroni F, Montone RA, et al. Ischemic Cardiomyopathy and Heart Failure After Acute Myocardial Infarction. Curr Cardiol Rep 2022;24:1505-15.

9. He S, Zhang Z, Luo R, et al. Advances in Injectable Hydrogel Strategies for Heart Failure Treatment. Adv Healthc Mater 2023;12:e2300029.

10. Wang RM, Christman KL. Decellularized myocardial matrix hydrogels: In basic research and preclinical studies. Adv Drug Deliv Rev 2016;96:77-82.

11. Ruvinov E, Cohen S. Alginate biomaterial for the treatment of myocardial infarction: Progress, translational strategies, and clinical outlook: From ocean algae to patient bedside. Adv Drug Deliv Rev 2016;96:54-76.

12. Zhang J, Guo Y, Bai Y, et al. Application of biomedical materials in the diagnosis and treatment of myocardial infarction. J Nanobiotechnology 2023;21:298.

13. Hu W, Yang C, Guo X, et al. Research Advances of Injectable Functional Hydrogel Materials in the Treatment of Myocardial Infarction. Gels 2022;8:423.

14. Lee RJ, Hinson A, Bauernschmitt R, et al. The feasibility and safety of Algisyl-LVR™ as a method of left ventricular augmentation in patients with dilated cardiomyopathy: initial first in man clinical results. Int J Cardiol 2015;199:18-24.

15. Sabbah HN, Wang M, Gupta RC, et al. Augmentation of left ventricular wall thickness with alginate hydrogel implants improves left ventricular function and prevents progressive remodeling in dogs with chronic heart failure. JACC Heart Fail 2013;1:252-8.

16. Anker SD, Coats AJ, Cristian G, et al. A prospective comparison of alginate-hydrogel with standard medical therapy to determine impact on functional capacity and clinical outcomes in patients with advanced heart failure (AUGMENT-HF trial). Eur Heart J 2015;36:2297-309.

17. Mann DL, Lee RJ, Coats AJ, et al. One-year follow-up results from AUGMENT-HF: a multicentre randomized controlled clinical trial of the efficacy of left ventricular

augmentation with Algisyl in the treatment of heart failure. Eur J Heart Fail 2016;18:314-25.

18. Wang B, Lee RJ, Tao L. First-in-human transcatheter endocardial alginate-hydrogel implantation for the treatment of heart failure. Eur Heart J 2023;44:326.

19. Tous E, Purcell B, Ifkovits JL, et al. Injectable acellular hydrogels for cardiac repair. J Cardiovasc Transl Res 2011;4:528-42.

20. Tous E, Ifkovits JL, Koomalsingh KJ, et al. Influence of injectable hyaluronic acid hydrogel degradation behavior on infarction-induced ventricular remodeling. Biomacromolecules 2011;12:4127-35.

21. Landa N, Miller L, Feinberg MS, et al. Effect of injectable alginate implant on cardiac remodeling and function after recent and old infarcts in rat. Circulation 2008;117:1388-96.

22. Wu B, Liu DA, Guan L, et al. Stiff matrix induces exosome secretion to promote tumour growth. Nat Cell Biol 2023;25:415-24.

23. Guo Y, Qiao Y, Quan S, et al. Relationship of matrix stiffness and cell morphology in regulation of osteogenesis and adipogenesis of BMSCs. Mol Biol Rep 2022;49:2677-85.

24. Wei J, Yao J, Yan M, et al. The role of matrix stiffness in cancer stromal cell fate and targeting therapeutic strategies. Acta Biomater 2022;150:34-47.

25. Wan W, Cheng B, Zhang C, et al. Synergistic Effect of Matrix Stiffness and Inflammatory Factors on Osteogenic Differentiation of MSC. Biophys J 2019;117:129-42.

26. Xing X, Wang Y, Zhang X, et al. Matrix stiffness-mediated effects on macrophages polarization and their LOXL2 expression. FEBS J 2021;288:3465-77.

27. Meli VS, Atcha H, Veerasubramanian PK, et al. YAP-mediated mechanotransduction tunes the macrophage inflammatory response. Sci Adv 2020;6:eabb8471.

28. Wang Y, Shi R, Zhai R, et al. Matrix stiffness regulates macrophage polarization in atherosclerosis. Pharmacol Res 2022;179:106236.

29. Wang J, Xie SA, Li N, et al. Matrix stiffness exacerbates the proinflammatory responses of vascular smooth muscle cell through the DDR1-DNMT1 mechanotransduction axis. Bioact Mater 2022;17:406-24.

30. Gao E, Lei YH, Shang X, et al. A novel and efficient model of coronary artery ligation and myocardial infarction in the mouse. Circ Res 2010;107:1445-53.

31. Berggård I, Bearn AG. Isolation and properties of a low molecular weight beta-2-globulin occurring in human biological fluids. J Biol Chem 1968;243:4095-103.

32. Trowsdale J, Knight JC. Major histocompatibility complex genomics and human disease. Annu Rev Genomics Hum Genet 2013;14:301-23.

33. Hansson GK. Inflammation, atherosclerosis, and coronary artery disease. N Engl J Med 2005;352:1685-95.

34. Chronic Kidney Disease Prognosis Consortium, Matsushita K, van der Velde M, et al. Association of estimated glomerular filtration rate and albuminuria with all-cause and cardiovascular mortality in general population cohorts: a collaborative meta-analysis. Lancet 2010;375:2073-81.

35. Amighi J, Hoke M, Mlekusch W, et al. Beta 2 microglobulin and the risk for cardiovascular events in patients with asymptomatic carotid atherosclerosis. Stroke 2011;42:1826-33.

36. Jin YX, Zhang S, Xiao J, et al. Association between serum β(2)-microglobulin levels and the risk of all-cause and cardiovascular disease mortality in chinese patients undergoing maintenance hemodialysis. BMC Nephrol 2023;24:170.

37. Shi F, Sun L, Kaptoge S. Association of beta-2-microglobulin and cardiovascular events and mortality:

38. Fang H, Zhang Q, Jin L. Association of beta-2-microglobulin with cardiovascular and all-cause mortality in the general and non-CKD population. Medicine (Baltimore) 2023;102:e33202.

39. Zhang B, Chen X, Mu X, et al. Serum Beta-2 Microglobulin: A Possible Biomarker for Atrial Fibrillation. Med Sci Monit 2021;27:e932813.

40. Vraetz T, Ittel TH, van Mackelenbergh MG, et al. Regulation of beta2-microglobulin expression in different human cell lines by proinflammatory cytokines. Nephrol Dial Transplant 1999;14:2137-43.

41. Cooper EH, Forbes MA, Hambling MH. Serum beta 2-microglobulin and C reactive protein concentrations in viral infections. J Clin Pathol 1984;37:1140-3.

42. Althubiti M, Elzubier M, Alotaibi GS, et al. Beta 2 microglobulin correlates with oxidative stress in elderly. Exp Gerontol 2021;150:111359.

43. Molenaar B, Timmer LT, Droog M, et al. Single-cell transcriptomics following ischemic injury identifies a role for B2M in cardiac repair. Commun Biol 2021;4:146.

A systematic review and meta-analysis. Atherosclerosis 2021;320:70-8.

Appendix 1

All animals

Forty-six mice (25±2 g, n=46) were numbered from 1 to 46 and a random number generation method was used to select 6 mice from the numbered list as the sham surgery group, while the remaining 40 were assigned to the surgery group.

Survival of mice

Among the 40 mice that underwent coronary artery ligation surgery, one died during the operation due to ventricular fibrillation. The remaining 39 mice were randomly assigned to the MI, MI + Saline, and MI + Hydrogels groups, with 13, 14, and 12 mice in each group, respectively. One mouse in the MI group died within 1 week after surgery, and 38 mice survived for 28 days with a survival rate of 95%. The sham surgery group had no deaths and a 100% survival rate.

mRNA sequencing

Three mice from each of the MI + Saline and MI + Hydrogels groups were randomly selected for mRNA sequencing.

Echocardiography

6, 12, 11, and 9 mice were left in the Sham, MI, MI + Saline, and MI + Hydrogels groups, respectively, for echocardiography.

RNA extraction, histological analysis and fluorescence immunohistochemistry assay

Four mice from each group were selected for RNA extraction, while the remaining mice were used for tissue sectioning and immunofluorescent staining. Due to the insufficient number of mice in the sham surgery group, we added 5 mice that received the same treatment as the sham surgery group for experimental analysis.

Randomisation

We utilized a pseudorandom number generator in R language to randomly assign 38 surviving mice to MI, MI + Saline, and MI + Hydrogels groups.

Firstly, we numbered the mice from 1 to 38 and randomly shuffled the numbers using the sample function. Then, we allocated the mice to three groups and employed a random number generation method to perform the grouping. Specifically, we utilized a loop to randomly shuffle the mouse numbers in each iteration and calculated the number of mice in each group. If the difference in the number of mice between any two groups did not exceed 1, we returned the grouping result.

Blinding

For each animal, three different investigators were involved as follows: a first investigator performed the relevant experiments according to random groups. This investigator was the only person aware of the treatment group allocation. A second investigator was responsible for the anaesthetic procedure. A third investigator (also unaware of treatment) assessed postoperative myocardial infarction in each group of mice.